Electronic Supplementary Information

Additive engineered SnO_2-based electron transport layer for the robust and high-efficiency large-scale perovskite solar cell

Byeong Jo Kim[1†], Gabseok Seo[2†], Sua Park[3], Donghyeon Lee[3], Yanqi Luo[4], Sarah Wieghold[4], Min-cheol Kim[3], Gerrit Boschloo[1*]*

[1] Department of Chemistry − Angstrom Laboratory, Physical Chemistry, Box 523, Uppsala University SE-751 20 Uppsala, Sweden

[2] PSC R&D Dept, UniTest Inc. Pyeongtaek 17791, Republic of Korea

[3] School of Mechanical Engineering, Pusan National University, Busan 46241, Republic of Korea

[4] Advanced Photon Source, Argonne National Laboratory, Lemont, Illinois 60439, United States

Correspondence and request for materials should be addressed to M.-c. Kim and G. Boschloo

(email: mckim90@pusan.ac.kr, gerrit.boschloo@kemi.uu.se)

[†] These authors contributed equally to this work

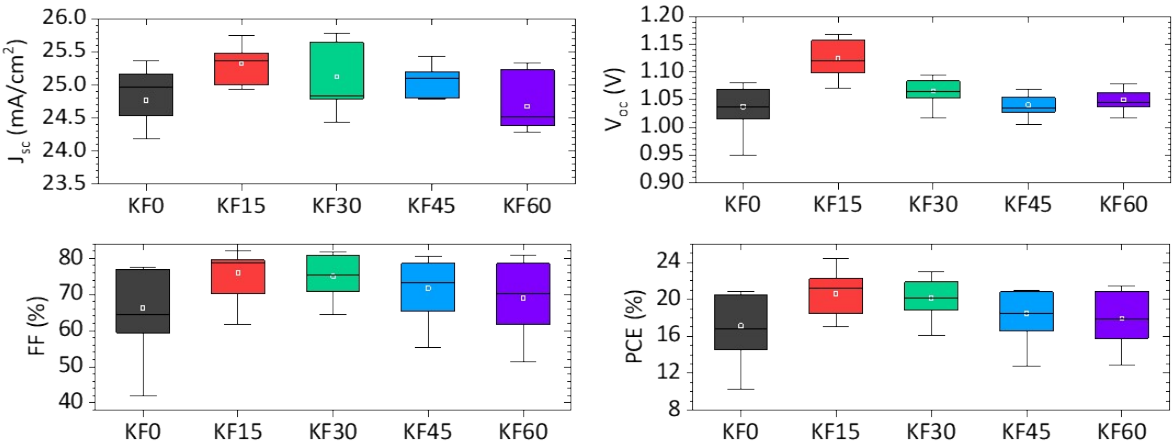

17

18 **Figure S1** The statistics box chart of (a) J_{sc}, (b) V_{oc}, (c) *FF*, and (d) PCE values obtained KF0,
19 KF15, KF30, KF45, and KF60:PSCs. The boxes show the standard deviations, n= 30; the
20 whiskers represent the 10/90 percentile; the small squares denote the mean, the two horizon
21 bars denote the 99 % and 1 % values.

22

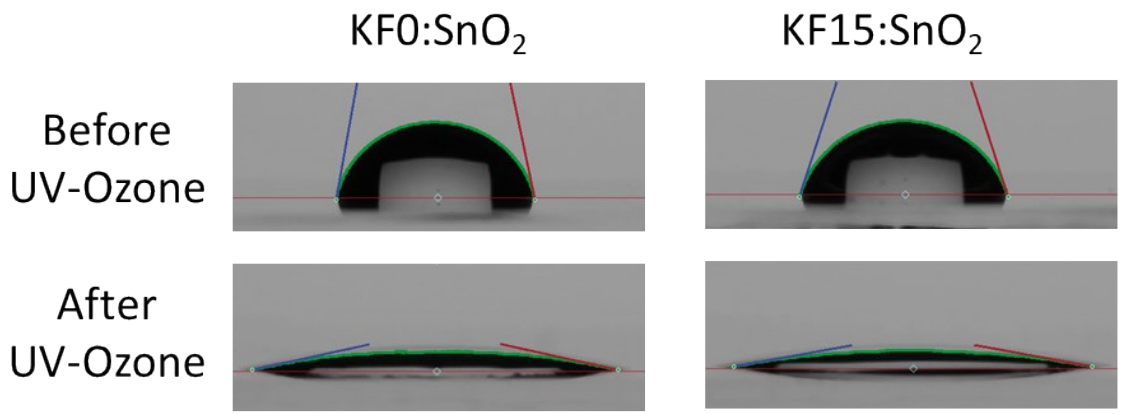

Figure S2 The images of (left) KF0, and (right) KF15:SnO_2 dispersion droplets on the FTO/glass substrate. The images of before/after UV-Ozone was taken at 80 seconds after dropping of droplet.

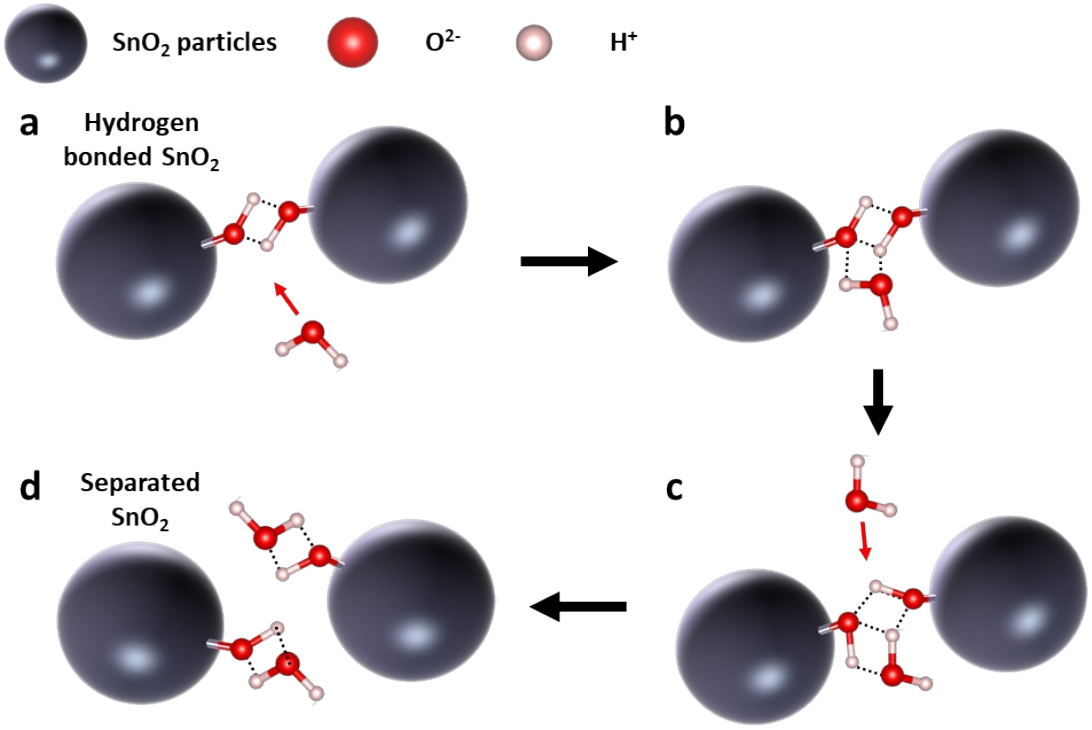

Figure S3 The schematic images present the interaction of aqueous SnO_2 colloidal system. (a) Hydroxyl radical caused hydrogen bonding within neighboring SnO_2. (b and c) When two free H_2O molecules approach to hydrogen bonding, hydrogen bonds are formed (d) The hydrogen bonds, which contribute to the agglomeration, are dissolved and the bonded SnO_2 particles get separated.

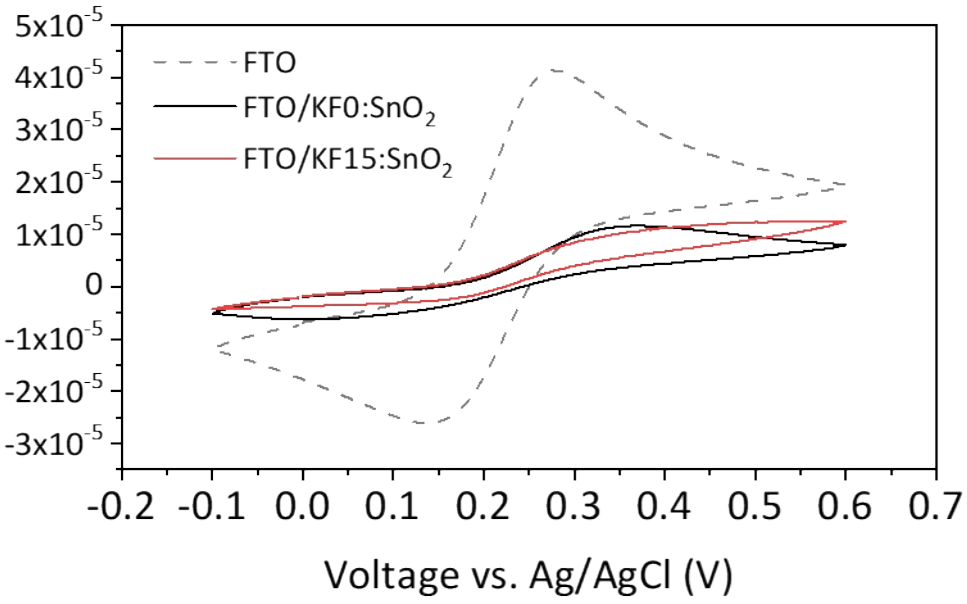

Figure S4 Cyclic voltammetry (CV) measurements for bare FTO, KF0:SnO_2, and KF15:SnO_2 films deposited on FTO in an aqueous solution of 1 mM $K_3Fe(CN)_6$, 1 mM $K_4Fe(CN)_6$ and 0.5 M KCl as the supporting electrolyte.

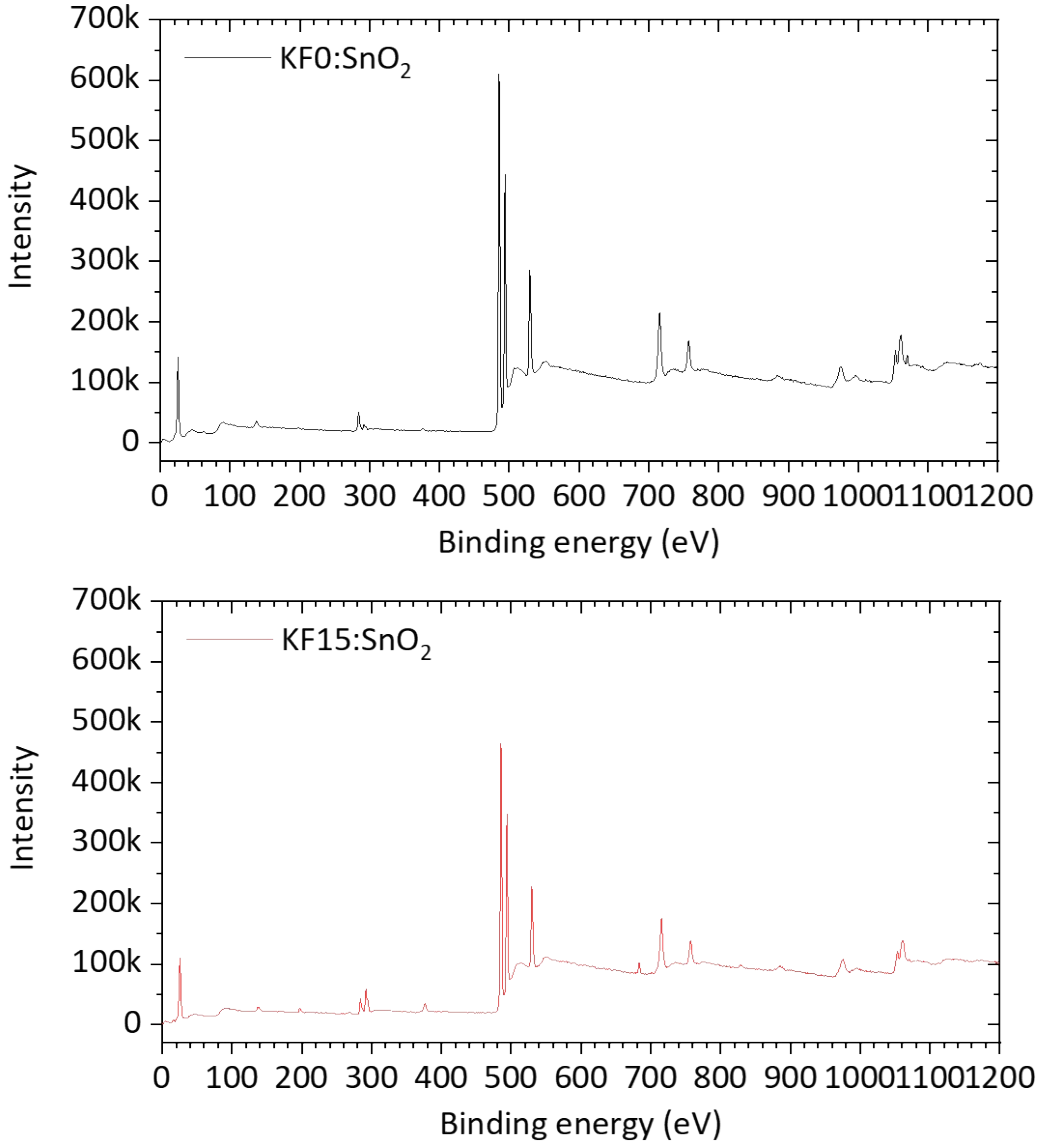

41

42 **Figure S5** Full spectra of X-ray photoemission spectroscopy measurements for (Top) KF0, and

43 (Bottom) KF15:SnO_2 films

44

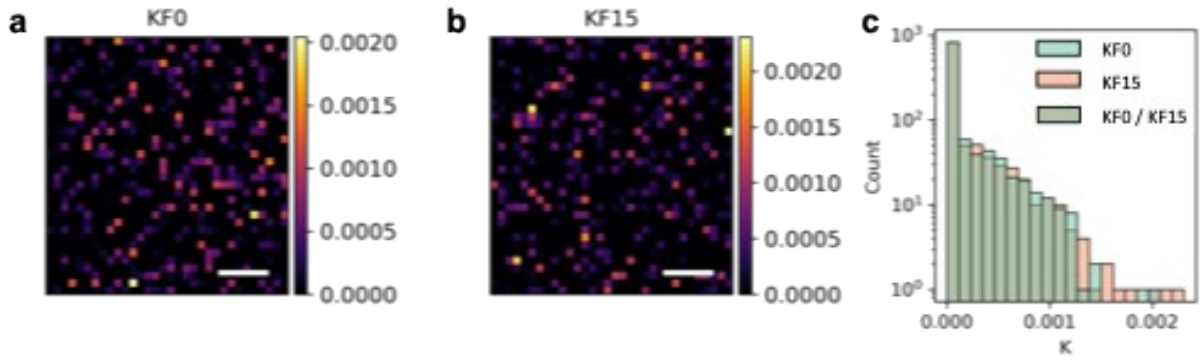

45

46 **Figure S6** X-ray fluorescence (XRF) mappings of elements (K) for (a) KF0:PSC and (b)
47 KF15:PSC. (c) K intensity counts for KF0:PSC and KF15:PSC. Legends for intensity counts
48 are KF0 (light green), KF15 (light red), KF0/KF15 overlapped (dark green). All scale bars are
49 2μm.

50

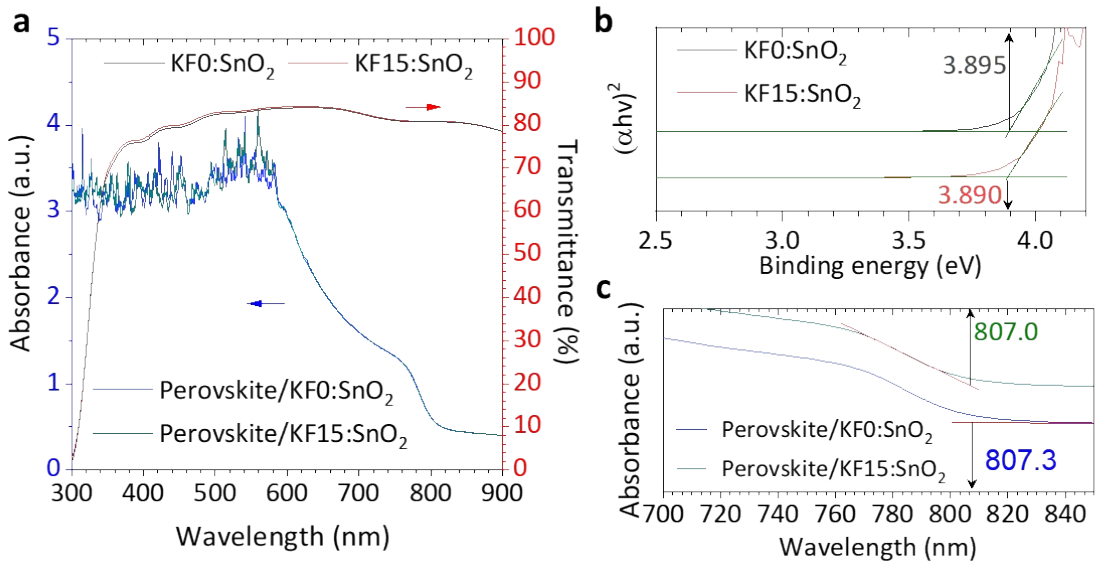

51

52 **Figure S7** (a) Absorption, transmission spectra, (b) Calculated Tauc's plot, and (c) absorption
53 cutoff for KF0:PSC and KF15:PSC.

54

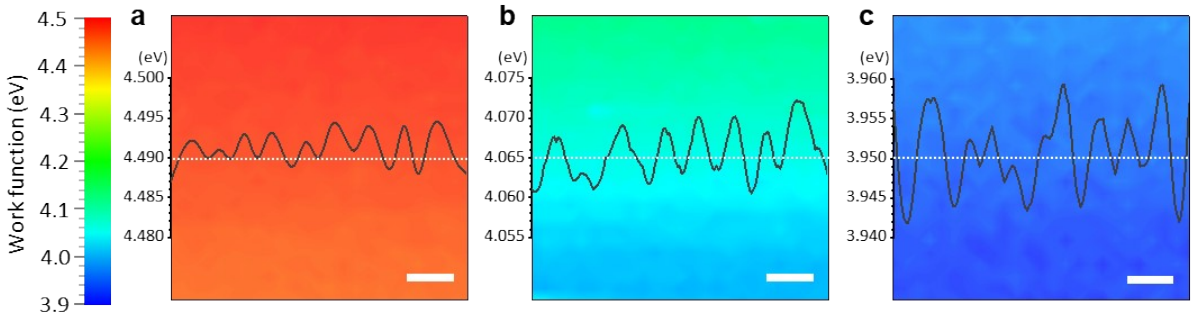

Figure S8 Kelvin probe forced microscopy mapping for FTO, KF0:SnO_2, and KF15:SnO_2. Scale bar indicates 5μm.

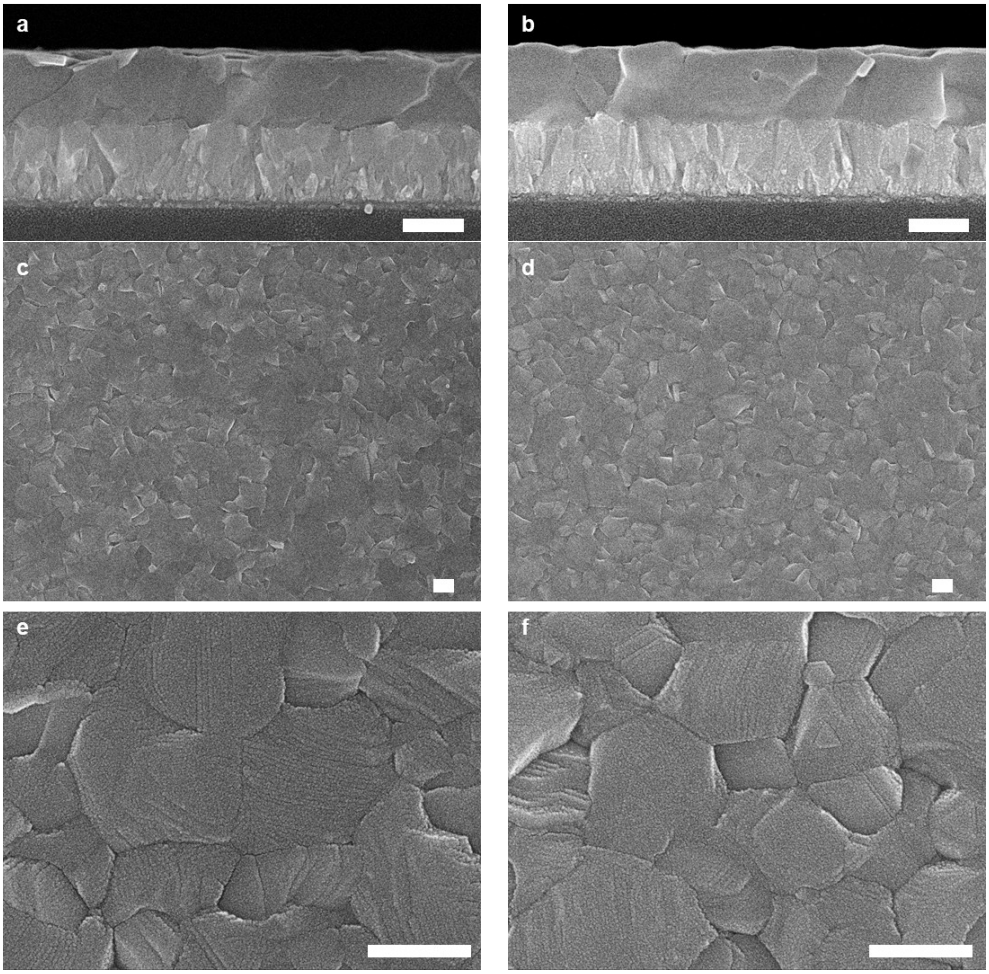

Figure S9 (a-b) Cross sectional, (c-d) plane-view, (e-f) zoomed-in plane-view scanning electron microscopic (SEM) images KF0:PSC and KF15:PSC. Scale bars indicate 500 nm.

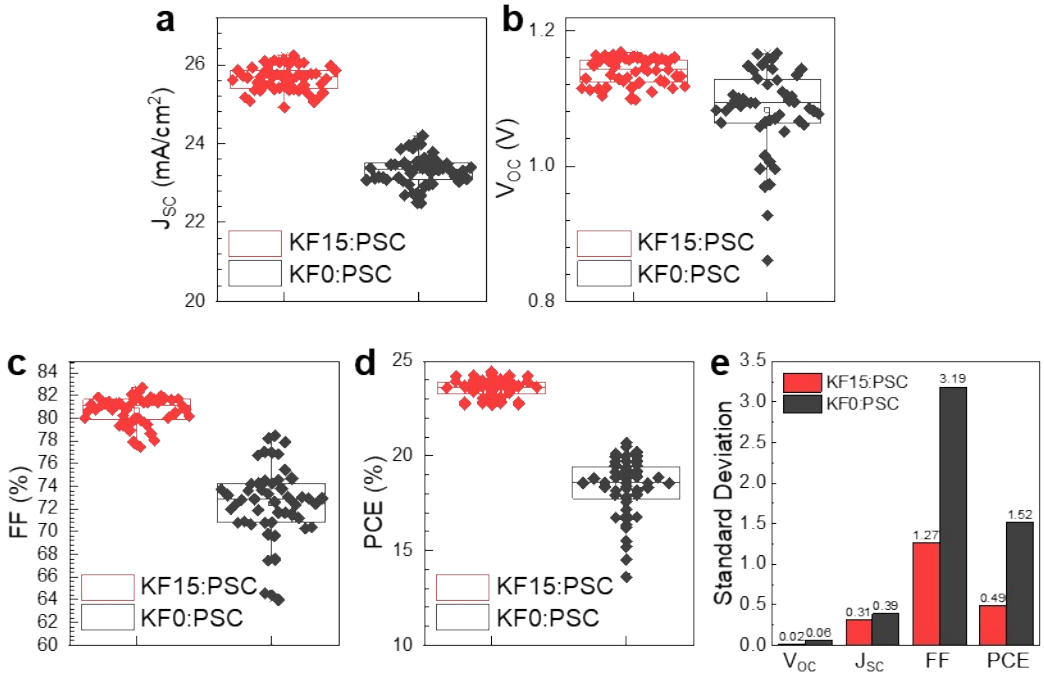

Figure S10 Statistic box plots of (a) J_{SC}, (b) V_{OC}, (c) FF and (d) PCE for 50 difference devices of optimized KF0:PSC and KF15:PSC. (e) Standard deviation values for each photovoltaic parameters for KF0:PSC and KF15:PSC.

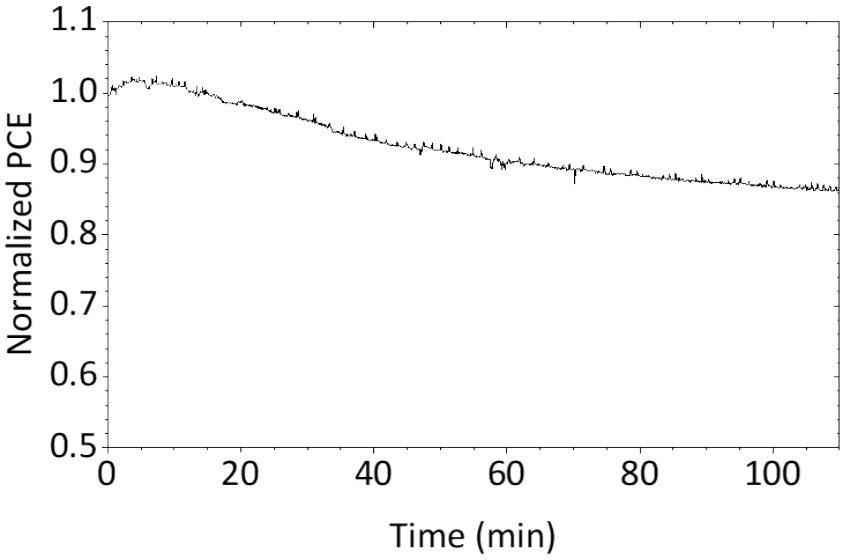

69

70 **Figure S11** Stabilized power output for champion devices using KF15:PSC.

71

72

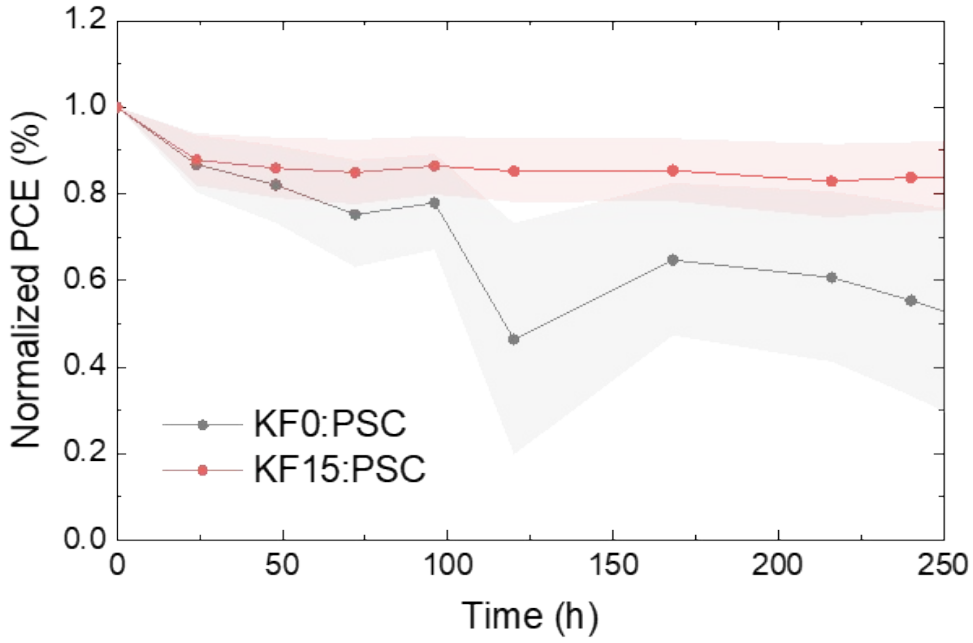

73

74 **Figure S12** Long-term stability test for KF0:PSC and KF15:PSC stored under the identical
75 60±5 % relative humidity condition.

76

	KF0	KF15	KF30
pH	11.35	11.18	11.14
Average Zeta potential (mV)	-46.7	-32.9	-33.4
Average Size (d.nm)	19.79	15.65	14.4

Table S1. Measured pH, zeta potential, and mean particle size of SnO_2 colloidal dispersion solution for KF0, KF15, and KF30.

Contact angle (°)	KF0			KF15		
	Left	**Right**	**Ave.**	**Left**	**Right**	**Ave.**
Before UV-Ozone	81.15	80.12	80.64	73.32	73.12	73.22
After UV-Ozone	12.52	12.65	12.59	10.47	10.67	10.57

Table S2. Measured contact angle for KF0 and KF15 SnO_2 dispersion solution on top of the FTO surface with and without UV-Ozone treatment.

Control SnO_2 (KF0:SnO_2)				
Component	**Binding Energy (eV)**	**FWHM (eV)**	**Atomic concentration (%)**	**Mass concentration (%)**
Sn $3d_{5/2}$	486.10	1.13	23.13±0.05	70.00±0.11
O 1s	530.00	1.30	50.28±0.29	20.50±0.15
K $2p_{3/2}$	292.50	1.37	2.22±0.05	2.04±0.05
F 1s	-	-	-	-
C 1s	284.49	1.19	24.38±0.31	7.46±0.11

Table S3. Binding energy peak, FWHM, atomic and mass concentration for each component derived from XPS measurement of KF0:SnO_2.

KF15:SnO_2				
Component	**Binding Energy (eV)**	**FWHM (eV)**	**Atomic concentration (%)**	**Mass concentration (%)**
Sn $3d_{5/2}$	485.87	1.16	21.54±0.15	64.87±0.19
O 1s	529.80	1.36	48.19±0.32	19.56±0.16
K $2p_{3/2}$	292.33	1.43	8.00±0.11	7.93±0.10
F 1s	684.19	1.32	4.85±0.11	2.34±0.05
C 1s	284.51	1.26	17.43±0.36	5.31±0.12

Table S4. Binding energy peak, FWHM, atomic and mass concentration for each component derived from XPS measurement of KF15:SnO_2.

(Unit: eV)	KF0:SnO_2	KF15:SnO_2	KF0:PSC	KF15:PSC
CBM	4.15	4.01	3.98	3.91
E_F	4.33	4.17	4.05	3.97
E_g	3.9	3.9	1.53	1.53
VBM	8.05	7.91	5.51	5.44

Table S5. Energy band level parameters (CBM, VBM, E_F, E_g) for KF0:SnO_2, KF15:SnO_2, KF0:PSC and KF15:PSC estimated by UPS and absorption spectra.

	Scan direction	J_{SC} (mA·cm^{-2})	V_{OC} (V)	FF (%)	PCE (%)	Hysteresis index
KF0:PSC	**Forward**	24.47	1.13	72.89	20.09	0.075
	Reverse	24.54	1.12	78.53	21.60	
KF15:PSC	**Forward**	25.66	1.16	80.71	24.21	0.010
	Reverse	25.75	1.16	81.76	24.46	

Table S6. Photovoltaic parameters of champion devices for KF0:PSC and KF15:PSC.

Samples	A_1 (%)	τ_1 (ns)	A_2 (%)	τ_2 (ns)	τ_{ave} (ns)
Glass/KF0:SnO_2	80.24	11.039	19.79	252.57	216.21
Glass/KF15:SnO_2	81.55	9.20	18.45	195.58	163.50

Table S7. Parameters of the TRPL Spectroscopy for Glass/KF0:SnO2/Perovskite and KF15:SnO2/Perovskite. The decay time and amplitude were fitted using bi-exponential decay equation: $y = y_0 + A_1 * exp\left(-\frac{x}{\tau_1}\right) + A_2 * exp\left(-\frac{x}{\tau_2}\right)$. Average decay time was estimated by using equation: $\tau_{avg} = \sum_i \tau_i A_i / \sum_i A_i$.

25cm² Aperture	Scan direction	J_{SC} (mA·cm^{-2})	V_{OC} (V)	FF (%)	PCE (%)
KF0:PSC Module	**Reverse**	20.8	11.40	74.46	17.70
	Forward	20.8	10.88	60.40	13.70
KF15:PSC Module	**Reverse**	22.9	10.84	72.47	18.02
	Forward	22.9	10.82	72.59	17.98

Table S8. Photovoltaic parameters of champion devices for KF0:PSC and KF15:PSC module fabricated with 25cm^2 aperture size.